Available online at www.sciencedirect.com
SCIENCE DIRECT®
Journal of Molecular Graphics and Modelling 22 (2003) 93–104
Journal of Molecular Graphics and Modelling
www.elsevier.com/locate/JMGM

2,3,7,8-Tetrachloro dibenzo-*p*-dioxin can be successfully decomposed over 2:1 dioctahedral smectite—a reactivity index study

Abhijit Chatterjee*, Takeo Ebina, Yoshio Onodera, Fujio Mizukami

Laboratory of Membrane Chemistry, National Institute of Advanced Industrial Science and Technology, AIST Tohoku, 4-2-1 Nigatake, Miyagino-ku, Sendai 983-8551, Japan

Accepted 17 March 2003

Abstract

2:1 Dioctahedral smectite family has shown its capability to decompose 2,3,7,8-tetrachloro dibenzo-*p*-dioxin (TeCDD) using the active hydroxyl hydrogen attached with the central octahedral aluminum, as monitored using density functional theory (DFT). From the values of the local softness and the charge on the hydrogen atom of the bridging/structural (occurring on the surface) hydroxyl attached to octahedral/tetrahedral metal site present in smectite used as a first approximation to the local hardness, it is concluded that the local acidities of the inorganic material systems are dependent on several characteristics which are of importance within the framework of hard–soft acid–base (HSAB) principle. The first step in this process of decomposition is the abstraction of chlorine bound to TeCDD using surface hydrogen of smectites. This results in non-chlorinated dibenzo-*p*-dioxin (NCDD), which is less toxic than TeCDD. The second step is the formation of a dative bond between oxygen of NCDD and hydroxyl proton of smectite, with the breaking of C–O bond of NCDD. The reaction mechanism is postulated within the helm of DFT using Fukui functions for all possible chlorinated and non-chlorinated dioxin varieties along with clay clusters. The material is identified to act for the decomposition of dioxin.

Keywords: Dioctahedral smectite; 2,3,7,8-Tetrachloro dibenzo-*p*-dioxin (TeCDD); Decomposition; DFT reactivity index

1. Introduction

Polychlorinated dibenzo-*p*-dioxins (PCDD)—highly toxic materials, have been detected as trace contaminants in municipal incinerators [1] and industrial heating facilities during combustion [2]. This become a serious global concern not only due to its acute and chronic toxicity, but also for their suspected role to act as endocrine disruptors that disturb the balance of hormones and damage the metabolism, immunity, and reproduction of exposed organisms [2,3]. Combustion processes, especially those of Municipal Solid Waste, are an important source of PCDD [4]. In countries, such as Switzerland [5], The Netherlands [6], Canada, and Japan [7], PCDDs are produced in municipal incinerators and industrial heating facilities during the combustion of chlorine-containing plastics. There have been many studies on the formation of dioxins under various conditions [8,9]. However, formation mechanisms were not yet completely understood because many parallel complex reaction pathways seemed to be involved in the process. One postulate, among many, has wide support from experiment, which is, formation of dioxin from precursors by a condensation reaction of two molecules of chlorophenols and the cyclization reaction of polychlorinated biphenyls [10,11]. Now, the disposal of PCDDs is still mainly based on high temperature incineration, which demands modification. We need a low energy process for dioxin decomposition. Although an understanding of the elementary processes involving formation of dioxin, their structure and other details will provide invaluable information, but the experiments are very hazardous due to the high toxicity of dioxin, hence molecular orbital calculations can help to rationalize the understanding.

There are many empirical and ab initio theoretical studies on PCDD [12–14]. The mechanism of the toxicity attributed to the PCDDs depends on structurally-related properties [13]. Fuji et al. [14] have studied the structure and energy of TCDD using the Gaussian 92 program at two ab initio molecular orbital levels: RHF/6-31G and RHF/6-31G*. These results are comparable with the structural information obtained from X-ray diffraction studies. There is a recent study on the formation of PCDDs by ab initio calculations [15]. They examined twelve possible pathways to locate the

* Corresponding author. Tel.: +81-22-237-5211; fax: +81-22-237-5217.
E-mail address: c-abhijit@aist.go.jp (A. Chatterjee).

1093-3263/03/$ – see front matter © 2003 Elsevier Science Inc. All rights reserved.
doi:10.1016/S1093-3263(03)00139-6

formation of TeCDD, the most toxic one among available 75 varieties of PCDD. They compared two possible pathways (1) by direct intermolecular condensation and (2) via direct radicals. They observed that TeCDD is the only one of the three PCDD isomers produced when the reactions proceed by direct condensation of trichloro phenol. On the other hand, when the reactions proceed through radicals, two path types seem to compete with each other. At low temperature, one path prefers to form TeCDD, but the other prefers to form phenoxy chloro dibenzo dioxin (PeCDD). Now, the destruction of dioxin by biological, chemical, or thermal means involves high costs, because it occurs in such low concentrations in the environment. Because of its high toxicity, there is no lower limit at which dioxin can be considered safe and would therefore require no remedial action. The desired concentration (i.e. threshold value for estimation) can be achieved through adsorption of the dioxin from solution onto a solid [16]. The optimal solid sorbent for dioxin should have the following properties: low cost, ease of handling, environmental neutrality, high affinity, high selectivity and the capability of being integrated into a dioxin-destruction process. Among many candidates examined experimentally, clays meet the majority of the above criteria.

Montmorillonite and beidellite is member of the 2:1 dioctahedral smectite family, which shares the common feature that two octahedral sites sandwich a sheet of octahedrally-coordinated metal ion. Substitution of a divalent metal ion for octahedral aluminum in montmorillonite and substitution of a trivalent metal ion for tetrahedral silicon in beidellite result in a net negative charge and an interaction with positive ions (exchangeable cation) to form an interlayer hydrated phase. Their activity lies in the layer charge resulting by either octahedral or by tetrahedral substitution. In any case, the hydroxyl hydrogen is attached with the octahedral metal ion through oxygen bridge or the structural hydroxyl occurring due to the substitution of tetrahedral ion in the active site of clay for catalytic activity [17].

The hard–soft acid–base (HSAB) principles classify the interaction between acids and bases in terms of global softness. Pearson proposed the global HSAB principle [18]. The global hardness was defined as the second derivative of energy with respect to the number of electrons at constant temperature and external potential, which includes the nuclear field. The global softness is the inverse of this. Pearson also suggested a principle of maximum hardness (PMH) [19], which states that, "for a constant external potential, the system with the maximum global hardness is most stable". In more recent days, density functional theory (DFT) has gained widespread use in quantum chemistry. Some DFT-based local properties, e.g. Fukui functions and local softness [20], have already been used for the reliable predictions in various types of electrophilic and nucleophilic reactions [21–24]. In our recent study [25], we proposed a reactivity index scale for heteroatomic interaction with zeolite framework. Moreover, Gazquez and Mendez [26] proposed that when two molecules, A and B of equal softness interact, it is implicitly assumed that one of the species is nucleophile and the other is an electrophile. Then, a novel bond would likely form between an atom A and an atom B whose Fukui function values are close to each other.

The aim of the current study is to find a material from the smectite family for the decomposition of dioxins. Two types of hydroxyl hydrogen present in the smectite in terms of tetrahedral and octahedral substitution are monitored. The location of hydroxyl hydrogen influences the activity of clay. The local reactivity index calculation is employed to find the perfect match between the interacting organic toxic pollutant starting form non-chlorinated (NCDD), mono-chlorinated (MCDD), di-chlorinated (DCDD), tri-chlorinated (TCDD) and tetrachlorinated (TeCDD) dioxin structures and smectite members. Montmorillonite type of clays with Mg^{2+} substituted for one of the octahedral Al^{3+} is compared with beidellite variety of clay where tetrahedral Si^{4+} is substituted with tetrahedral Al^{3+} to compare the effect of location of layer charge on the reaction process. A reactivity index scale is proposed in terms of activity of clay materials chosen. Based on that, the decomposition scenario has been proposed. The decomposition consists of two steps: (1) selective abstraction of chlorine from dioxins and (2) decomposition of dioxin ring by breaking the C–O bond of the molecule. The reactions are carried out in presence of the active hydroxyl hydrogen of clays. The current methodology rationally designs a material from the 2:1 dioctahedral smectite family suitable for decomposition of dioxin in a cheapest and environment friendly way.

2. Theory

Let us first recall the definition of various quantities employed. Parr and Yang [20] have demonstrated that most of the frontier electron theory of chemical reactivity can re rationalized from the DFT of the electronic structure of molecules. The Fukui function $f(r)$ is defined by [20]

$$f(r) = \left[\frac{\delta\mu}{\mathrm{d}v(r)}\right] N = \left[\frac{\delta\rho(r)}{\delta N}\right] v \tag{1}$$

The function 'f' is thus a local quantity, which has different values at different points in the species, N is the total number of electrons, μ the chemical potential, and v is the potential acting on an electron due to all nuclei present. Since $\rho(r)$ as a function of N has slope discontinuities, Eq. (1) provides the following three reaction indices [20]:

$$f^{-}(r) = \left[\frac{\delta\rho(r)}{\delta N}\right]^{-}_{v} \quad \text{(governing electrophilic attack)},$$

$$f^{+}(r) = \left[\frac{\delta\rho(r)}{\delta N}\right]^{+}_{v} \quad \text{(governing nucleophilic attack)},$$

$$f^{0}(r) = \tfrac{1}{2}[f^{+}(r) + f^{-}(r)] \quad \text{(for radial attack)}$$

In a finite difference approximation, the condensed Fukui function [27] of an atom, say x, in a molecule with N electrons are defined as

$$f_x^+ = [q_x(N+1) - q_x(N)] \quad \text{(for nucleophilic attack)},$$
$$f_x^- = [q_x(N) - q_x(N-1)] \quad \text{(for electrophilic attack)},$$
$$f_x^0 = \frac{[q_x(N+1) - q_x(N-1)]}{2} \quad \text{(for radical attack)} \qquad (2)$$

where q_x is the electronic population of atom x in a molecule. In density functional theory, hardness (η) is defined as [28]

$$\eta = \frac{1}{2}\left(\frac{\delta^2 E}{\delta N^2}\right) v(r) = \frac{1}{2}\left(\frac{\delta \mu}{\mathrm{d}N}\right)_v$$

The global softness, S, is defined as the inverse of the global hardness, η.

$$S = \frac{1}{2}\eta = \left(\frac{\delta N}{\delta \mu}\right)_v$$

The local softness $s(r)$ can be defined as

$$s(r) = \left(\frac{\delta \rho(r)}{\delta \mu}\right)_v \qquad (3)$$

Eq. (3) can also be written as

$$s(r) = \left[\frac{\delta \rho(r)}{\delta N}\right] v \left[\frac{\delta N}{\delta \mu}\right]_v = f(r)S \qquad (4)$$

Thus, local softness contains the same information as the Fukui function $f(r)$ plus additional information about the total molecular softness, which is related to the global reactivity with respect to a reaction partner, as stated in HSAB principle. Using the finite difference approximation, S can be approximated as

$$S = \frac{1}{IE - EA} \qquad (5)$$

where IE and EA are the first ionization energy and electron affinity of the molecule, respectively. Atomic softness values can easily be calculated by using Eq. (4), namely:

$$s_x^+ = [q_x(N+1) - q_x(N)]S,$$
$$s_x^- = [q_x(N) - q_x(N-1)]S,$$
$$s_x^0 = S\frac{[q_x(N+1) - q_x(N-1)]}{2} \qquad (6)$$

3. Computational methodology and model

In the present study, all calculations have been carried out with DFT using DMOL code of MSI Inc. [29]. A gradient corrected functional BLYP [30,31] and DNP basis set [32] were used throughout the calculation. Basis set superposition error (BSSE) was also calculated for the current basis set in non-local density approximation (NLDA) using Boys–Bernardi method [33]. Geometries of the interacting TeCDD/TCDD/DCDD/MCDD/NCDD along with the individual clay cluster models representing different isomorphous substitution in the octahedral aluminum/tetrahedral

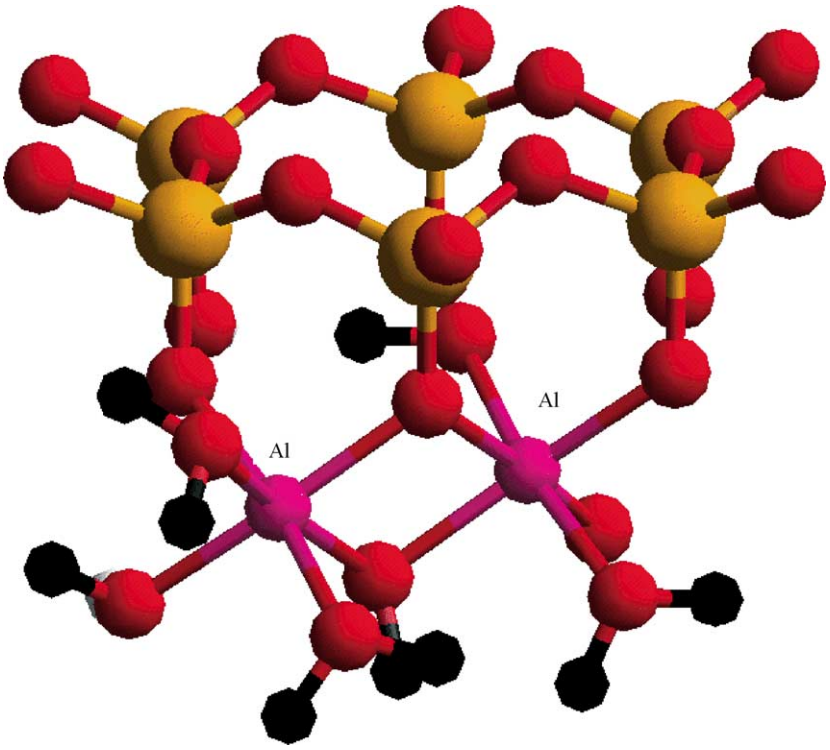

Fig. 1. The cluster model of montmorillonite with six tetrahedral silicons at the top and two octahedral aluminum atoms. It is the top view of the cluster. The aluminum atoms are labeled. The color code is as follows: red (oxygen); yellow (silicon); violet (octahedral aluminum); and black (hydrogen).

silicon of dioctahedral smectites were fully optimized for calculating the reactivity index. The theory for reactivity index calculations is mentioned in details elsewhere [25]. Single point calculations of the cation and anion of each molecule at the optimized geometry of the neutral molecule were also carried out to evaluate Fukui functions and global and local softness. The condensed Fukui function and atomic softness were evaluated using Eqs. (2) and (6), respectively. The gross atomic charges were evaluated by using the technique of electrostatic potential (ESP) driven charges.

The ideal formula of the clay montmorillonite, a member of 2:1 dioctahedral smectite family, is $(Na_x^+, nH_2O)(Al_{4-x}Mg_x)\ Si_8O_{20}\ (OH)_4$ [34]. The $Al_2Si_6O_{24}H_{18}$ cluster was generated from the clay structure as shown in Fig. 1.

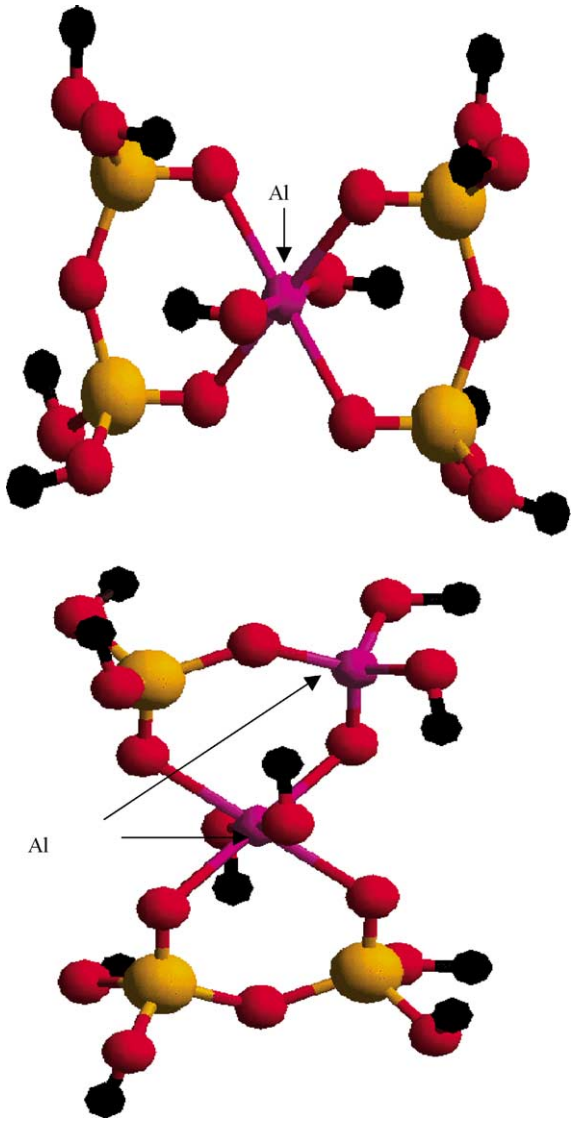

Fig. 2. The initial configuration of clay cluster having the formula (a) $TSi_4O_{14}H_{10}$ (representing montmorillonite) and (b) $AlSi_3AlO_{16}H_{11}$ (representing beidellite) is shown. The aluminum atoms are labeled. The color code is as follows: red (oxygen); yellow (silicon); violet (octahedral aluminum); and black (hydrogen).

Fig. 1 displays the top view of one tetrahedral and one octahedral sheet, showing the hexagonal cavities at the oxygen surface of the silicon layers. The dangling bonds were saturated with hydrogens, not shown in Fig. 1 for visual clarity. Two localized clusters were generated to represent two types of 2:1 dioctahedral smectite (a) montmorillonite and (b) beidellite. The clusters are having the formula $MgSi_4O_{16}H_{10}$ and $AlSi_3AlO_{16}H_{11}$, where the adjacent silicon and aluminum atoms occurring in the clay lattice are replaced by hydrogens to preserve the electroneutrality of the model. The clusters are shown in Fig. 2a and b, respectively. The varieties of dioxin molecule used in this study are shown in Fig. 3.

4. Results and discussion

The aim of the current communication is to monitor the decomposition of dioxin over 2:1 dioctahedral smectite. The two most commonly available varieties of smectite are chosen with different location of layer charge, which is responsible for its activity. The varieties of dioxin with different amount of chlorine present along with the different location of chlorine atom were explored to rationalize emphatically the chlorine abstraction process, the first step of dioxin decomposition. The activities of the dioxin counterpart were compared with clay clusters to locate the active site of clay interacting with the dioxin molecule. The electronic and structural properties of the dioxin and furan varieties along with the clay cluster models are first rationalized. The global softness values of the clay cluster models as well as the interacting molecules are calculated using DFT and are presented in Table 1. The values of nucleophilic condensed local softness (s_x^+) and condensed Fukui function (f_x^+) of the individual atoms of the clay cluster models obtained through ESP technique at DFT level is shown in Table 2. This is to compare between magnesium substituted montmorillonite and aluminum substituted beidellite variety. The values of electrophilic condensed local softness (s_x^-) and condensed Fukui function (f_x^-) of the major electrophilic centers of the dioxin molecules obtained through ESP technique at DFT

Table 1
Global softness values (in a.u.) for clay clusters and dioxin molecules

Molecules	Global softness (a.u.)
$[MgSi_4O_{16}H_{10}]^-$	1.52173
$AlSi_3AlO_{16}H_{11}$	2.22610
TeCDD	4.08804
238-TCDD	4.11557
237-TCDD	4.12066
28-DCDD	4.06369
23-DCDD	4.07273
27-DCDD	4.08535
8-MCDD	3.98444
2-MCDD	3.99440
NCDD	3.80055

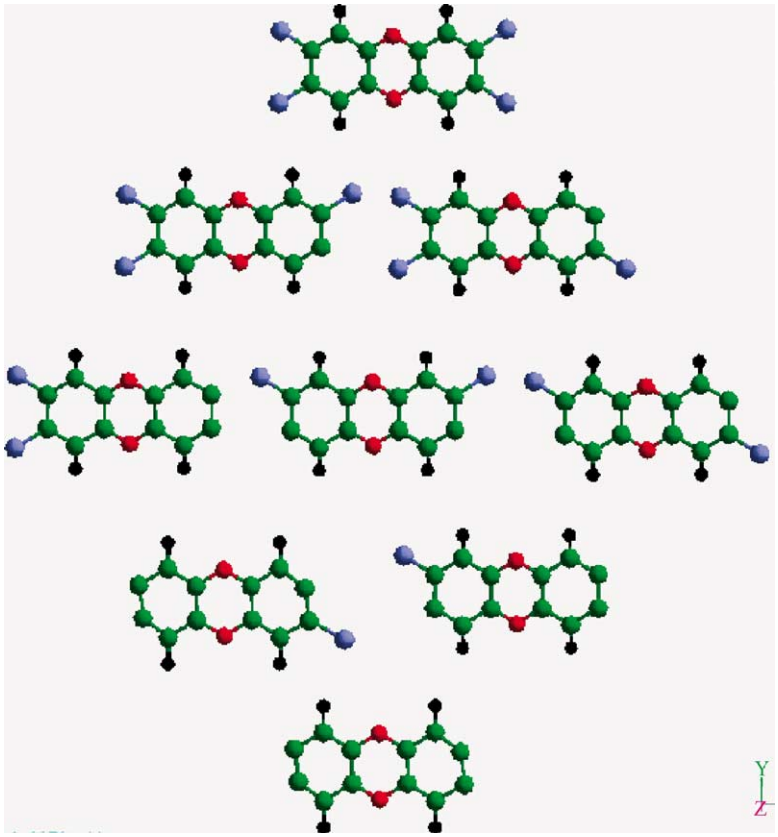

Fig. 3. The initial configurations of dioxin varieties are shown with the order from top: TeCDD, 237-TCDD, 238-TCDD, 23-DCDD, 27-DCDD, 28-DCDD, 8-MCDD, 2MCDD, and NCDD. The hydrogens after chlorine abstraction are not shown for visual clarity. The color code is as follows: green (carbon); red (oxygen); black (hydrogen); and blue (chlorine).

level is shown in Tables 3 and 4, respectively. It is observed from Table 1, that those global softness values for the clay cluster models are lower than that of the interacting molecular species. So to test the HSAB principle, it seems to be important to analyze whether the local softness values, Fukui functions or reactive indices for the constituent atoms of the cluster models and interacting molecular species, will be more reliable parameter. First, a qualitative trend is proposed in terms of the local reactivity descriptors in the helm of HSAB between the different clay clusters and the interacting molecules, to rationalize the phenomenon and to trace a selectivity of clays for the respective organic pollutants in terms of their active centers. This has been done by com-

Table 2
Condensed local softness and Fukui function values (a.u.) for clay clusters representing montmorillonite (with Mg^{2+} at octahedral position) and beidellite (with Al^{3+} at tetrahedral position)

Atoms	Substituent cation for tetrahedral Si^{4+} and octahedral Al^{3+}			
	Mg^{2+} (for octahedral Al^{3+})		Al^{3+} (for tetrahedral Si^{4+})	
	f_x^+	s_x^+	f_x^+	s_x^+
T1	0.150	0.229	0.219	0.487
Si	0.058	0.089	0.090	0.200
O-structural	0.061	0.093	0.234	0.520
O-hydroxyl	0.402	0.612	0.170	0.378
O-hydroxyl	0.458	0.698	0.187	0.416
H-structural	0.016	0.025	0.302	0.672
H-hydroxyl	0.323	0.492	0.168	0.373
H-hydroxyl	0.396	0.603	0.172	0.382

T1: Substituent cation Mg^{2+}(for octahedral Al^{3+}) and Al^{3+}(for tetrahedral Si^{4+}) for montmorillonite and beidellite, respectively.

Table 3
Condensed local softness and Fukui function values (a.u.) for the main active centers (chlorine and oxygen) present in different dioxin varieties

Atoms	Active centers present in dioxin varieties			
	Chlorine atom center		Oxygen atom center	
	f_x^-	s_x^-	f_x^-	s_x^-
TeCDD	0.111	0.457	0.051	0.208
238-TCDD	0.205	0.846	0.046	0.192
237-TCDD	0.213	0.881	0.045	0.187
28-DCDD	0.245	1.063	0.046	0.188
23-DCDD	0.253	1.032	0.045	0.185
27-DCDD	0.261	1.004	0.044	0.183
8-MCDD	0.322	1.286	0.046	0.185
2-MCDD	0.293	1.173	0.048	0.191
NCDD			0.045	0.159

paring the nucleophilicity and electrophilicity of the interacting centers of the interacting molecules to trace the steps of the reaction of decomposition process. This order is validated by the interaction energy calculations. Now here, in the clay cluster two different types of hydroxyl has been observed (1) is the structural hydroxyl present during a tetrahedral substitution occurred in beidellite variety of clay and (2) hydroxyl hydrogen attached with octahedral metal cation present in montmorillonite variety. The orientation of the optimized interacting molecular conformation is also monitored to justify its inter-molecular interaction with octahedral/tetrahedral metal ion present in the clay framework.

4.1. Activity of clay cluster and interacting dioxin molecules in terms of reactivity index

In order to choose the best material suitable for decomposition of dioxin from the 2:1 dioctahedral clay structures first we need to know the active center present in it. Now, for montmorillonite, Mg^{2+} replaces one of the Al^{3+} ions present at octahedral site and for beidellite, tetrahedral Si^{4+} is replaced by Al^{3+}, to monitor the role of octahedral/tetrahedral substitution on the sorption of those organic molecules mentioned previously. In each case, the cluster was totally optimized. The initial configurations of the representative clusters are shown in Fig. 2a and b, respectively. We compared the localized properties in terms of Fukui function and local softness for the octahedral magnesium-substituted cluster representing montmorillonite with tetrahedral aluminum-substituted cluster representing beidellite. The aim is to compare the activity of structural and bridging hydroxyl hydrogen present in the clay structure. The results are shown in Table 2. The results show that for a situation with tetrahedral Al^{3+} substitution, the surface hydroxyl is more active than the bridging hydroxyl attached to octahedral aluminum. This is because the layer charge of beidellite is originated from the tetrahedral substitution and not from octahedral substitution. Now, combining the activities of these two sets of clay clusters, it was found that the order of activity in terms of hydroxyl hydrogen montmorillonite is more active than beidellite type of clays, whereas, the reverse is true for structural hydroxyl group. The global softness values showed that octahedral Mg^{2+}-containing cluster has a lower value than that of tetrahedral Al^{3+} substituted one. At this point, the results show that the hydroxyl hydrogens of 2:1 smectite clays may behave as a nucleophilic center. In route to find the suitable decomposer for dioxin, we need to know the activity of dioxin molecules as well to find a match in the domain of HSAB principle.

Now, for dioxin molecules, we have chosen all possible varieties of dioxin in terms of chlorine atom content and its location. It is observed from the global softness values that the global softness decreases with decreasing number of chlorine atoms present. The value is the lowest for NCDD. The values are not quantitative. But still the numbers raise a question about the role of the numbers and locations of chlorine atoms present in dioxin varieties. As these numbers do not incorporate any insight into the electronic structure of the molecules, local properties certainly would contain more information. So we calculated the local atomic softness (s_x^-) values and Fukui function (f_x^-) for the constituent atoms of all the dioxin varieties using ESP method with DFT, and these results of the active atoms are shown in Table 3. Two of the most probable active centers present in dioxin molecule (1) the chlorine atoms and (2) the oxygen atoms are monitored. The results show that the local softness values for the chlorine atom for all the dioxin varieties are much higher in comparison to the oxygen centers present. The order of activity of is as follows:

For chlorine as the electrophilic center:

$$\text{8-MCDD} > \text{2-MCDD} > \text{28-DCDD} > \text{23-DCDD} > \text{27-DCDD} > \text{237-TCDD} > \text{238-TCDD} > \text{TeTCDD}.$$

For oxygen as the nucleophilic center:

$$\text{TeTCDD} > \text{238-TCDD} > \text{237-TCDD} > \text{27-DCDD} > \text{23-DCDD} > \text{28-DCDD} > \text{2-MCDD} > \text{8-MCDD} > \text{NCDD}.$$

NCDD shows the lowest local softness for the oxygen atom. The oxygen of TeTCDD has the highest local softness value. This suggests that the number of chlorine atoms present in the dioxin varieties influences the local softness values. Hence, the chlorine of MCDD is the most electrophilic, and it follows in an order from TeCDD to MCDD. So we can propose that chlorine abstraction from dioxin can be a stepwise process and lead NCDD. The results for oxygen center depict the same story from the other direction. The oxygen of TeCDD shows the highest value, which is again dependent on the number of chlorine atoms present and thus with abstraction of chlorine, the values fall in an order so as to end with NCDD. Therefore, the lowest value component will trigger the decomposition process; TeCDD will first interact with its nucleophilic counterpart to start the chlorine abstraction process, whereas the NCDD oxygen will interact with its match in search for the C–O bond breaking partner. Now to trace the decomposition mechanism, we need to find comparable nucleophilic activity from the clay varieties. This will help us to postulate the interaction scenario. At this point, we may propose that chlorine abstraction can be the first step of the decomposition reaction.

4.2. Reactivity index scale

The aim of the current study is to find a material from smectite family suitable for dioxin decomposition through a process, which will proceed via first chlorine abstraction followed by C–O bond dissociation. We have used two sets of clay clusters to monitor the role of different types of

hydroxyl hydrogen present in the clay cluster. It is observed that in terms of global softness values dioxin varieties have higher values in comparison to the clay clusters. NCDD has the lowest value among dioxin varieties and cluster representing montmorillonite type clay has the lowest value in comparison to the other cluster representing beidellite. The order of global softness for dioxin varieties is as follows: NCDD < 8-MCDD < 2-MCDD < 28-DCDD < 23-DCDD < 27-DCDD < TeCDD < 237-TCDD < 238-TCDD. The order of global softness of for representative clay clusters is as follows:

Al^{3+} (substituted at tetrahedral Si^{4+})
> Mg^{2+} (substituted at octahedral Al^{3+})

Now, we present the results of the condensed local softness and Fukui functions of the most nucleophilic atom of the cluster from ESP techniques in Table 2. The results show that both in terms of Fukui functions and condensed local softness, the hydroxyl hydrogen attached to octahedral Mg^{2+} in clay cluster representing montmorillonite type clay is more active in comparison to hydroxyl hydrogen attached to octahedral Al^{3+} in beidellite type clay cluster, whereas the trend is reversed for structural hydrogen. This can be correlated with the location of layer charge. The layer charge resulted in montmorillonite type clay from octahedral substitution, and hence the higher softness values for hydroxyl hydrogen and in case of beidellite type the layer charge are due to the tetrahedral substitution. At the same time, it is observed from local softness values that for beidellite the hydrogen activities are comparable with each other (structural and hydroxyl), whereas for montmorillonite, the activity of structural hydroxyl is very low compared to the hydroxyl hydrogen. In order to monitor the match between the local softness of the electrophilic centers of the organic toxic molecules to that of nucleophilic center of the clay clusters, we calculated the ratio of s_x^+ and s_x^-. This ratio is thus a ratio of the local softness of most nucleophilic center of clay cluster to the local softness value of most electrophilic center of the dioxin moiety. This idea has been first proposed by Roy et al. [35] to predict intramolecular and intermolecular reactivity sequences of carbonyl compounds. We have used this ratio to find the best dioctahedral smectite for nitrogen heterocyclics adsorption [36]. The results are shown in Figs. 4 and 5. It is observed that for the interaction between chlorine center of dioxin molecules and hydroxyl/structural hydrogen of clay clusters, for montmorillonite type clays, the ratio of s_x^+ and s_x^- is perfect one for TeCDD and gradually decreases for the rest in the order TeCDD < 238-TCDD < 237-TCDD < 27-DCDD < 23-DCDD < 28-DCDD < 2-MCDD < 8-MCDD. The trend is same but with a higher value for all of the set of dioxin molecules with the highest being with TeTCDD. The results are shown in Fig. 4. Fig. 5 shows the trend for the interaction between oxygen centers of dioxin molecules with nucleophilic centers of clay clusters. The ratio of s_x^- and s_x^+ are plotted. The results show an opposite trend, here the values for montmorillonite are higher compared to beidellite, and for the dioxin set in both the cases, the TeTCDD has a higher relative nucleophilicity with NCDD being lowest. The order remains the same as above with an addition of NCDD at the end: TeTCDD < 238-TCDD < 237T-TCDD < 27-DCDD < 23-DCDD < 28-DCDD < 2-MCDD < 8-MCDD < NCDD. The results show another point that surface hydroxyl may interact favorably with chlorine atom of dioxin, and the hydroxyl hydrogen will have a favorable interaction with oxygen center. The trend also shows that an oxygen interaction is less favorable in comparison to that of a chlorine interaction. This is due to the fact that the oxygen center is less active than its chlorine counterpart. Hence, chlorine will first interact with clay and then with oxygen. In that case, NCDD has a more feasible chance of interaction with clay. Though the trend is qualitative, the information generated from the trend is invaluable. The varieties of 2:1 smectite will help in the successful abstraction of chlorine in steps through TCDD, DCDD, MCDD and NCDD. Once NCDD is formed, this

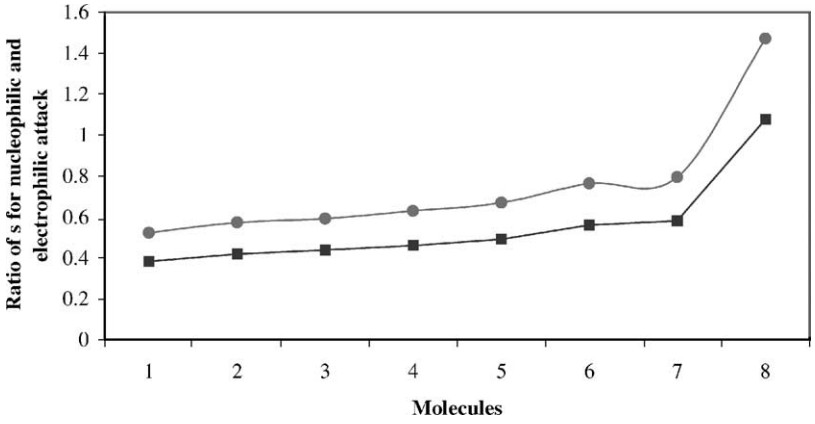

Fig. 4. Ratio of local softness values for nucleophilic H of clay clusters both montmorillonite (■) and beidellite (●) to that of electrophilic Cl of different dioxin varieties is plotted against each of the interacting organic toxic molecules. The molecules are represented as follows: (1) 8-MCDD, (2) 2-MCDD, (3) 28-DCDD, (4) 23-DCDD, (5) 27-DCDD, (6) 237-TCDD, (7) 238-TCDD, and (8) TeCDD.

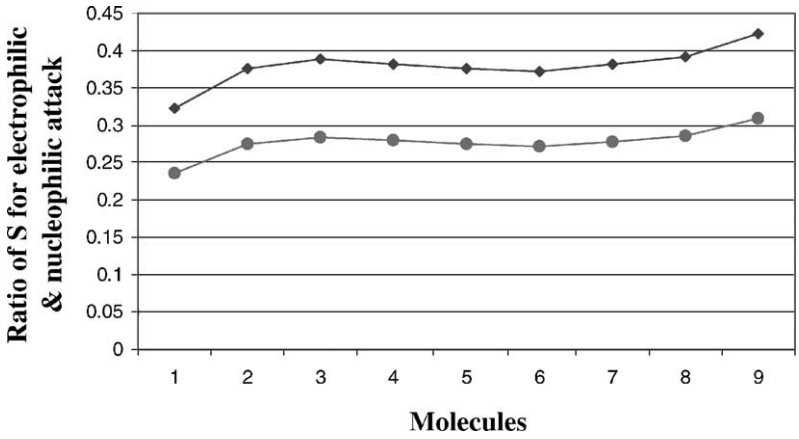

Fig. 5. Ratio of local softness values for nucleophilic H of clay clusters both montmorillonite (◆) and beidellite (●) to that of electrophilic O of different dioxin varieties is plotted against each of the interacting organic toxic molecules. The molecules are represented as follows: (1) 8-MCDD, (2) 2-MCDD, (3) 28-DCDD, (4) 23-DCDD, (5) 27-DCDD, (6) 237-TCDD, (7) 238-TCDD, and (8) TeCDD.

moiety can then interact with nucleophilic center of clay through its oxygen center for the second step of the decomposition process. To visualize now the orientation of the interacting molecule and the interaction process, interaction energy calculations have been performed to locate the bond dissociation process.

4.3. Dioxin decomposition process

As mentioned before, the dioxin decomposition is a two-step process with the first step being chlorine abstraction, followed by decomposition through bond breaking and formation. A recent paper of Okamoto et al. [15] on the formation pathways of three PCDD isomers from 2,4,5-trichlorophenol (TCP) showed that chlorine abstraction from a benzene ring of TCP, through the irradiation of hydrogen radical, is more favorable than hydrogen abstraction from the ring both thermodynamically and kinetically. This gives us a feeling about our approach. We proceeded through the following game plan as our first target is to monitor the chlorine abstraction process, the reaction is as follows:

(a) for montmorillonite : $MgSi_4O_{16}H_{10}$ + chloro dioxins = $MgSi_4O_{16}H_9 + HCl$
(b) for beidellite : $AlSi_3AlO_{16}H_{11}$ + chloro dioxin = $AlSi_3AlO_{16}H_{10} + HCl$

Now, from the reactivity index calculations we have observed that the structural hydroxyls are more active in beidellite in comparison to montmorillonite; while the reverse is true for hydroxyl hydrogen. The results find support in terms of the hydrogen bond formation between water and a hydroxyl proton present in montmorillonite as mentioned in an IR study [37]. Sposito et al. [37] have proposed that in case of smectites, which have their isomorphous substitution in the tetrahedral sheet, water molecules are involved in hydrogen bonding with oxygen atoms belonging to the tetrahedral aluminum which were replaced by tetrahedral silicon. From the relative nucleophilicity calculation, it is observed that chlorine abstraction is more feasible process in beidellite, though montmorillonite has some selectivity. The only constraint with that of montmorillonite is that the structural hydrogen has no role in the interaction process with dioxin. So, if TeCDD has to interact with hydroxyl hydrogen, it needs to pass through the hexagonal hole of the clay surface as shown in Fig. 1. Though an earlier work of Fuji et al. [14] has shown that dioxin molecules have a butterfly-like movement around the central axis along the central oxygen atoms of the dioxin molecule. Still this is much less favorable for dioxin molecule to enter the montmorillonite layer, as surface silanols are present on clay surface. As we observed that beidellite having higher surface interaction possibilities with dioxin, which make this material as a potential candidate for the decomposition process, we carried out the interaction energy calculations with beidellite. Each of the dioxin varieties with the chlorine pointed towards surface hydroxyl is optimized with an initial Cl–H distance being 3.0 Å. Then the bonded atom was moved closer manually with an initial interval of 0.5 Å, followed by 0.2 Å distant. Each structure at that distance was fully relaxed, and thus a potential energy surface was generated. Chlorine abstraction seems to be a more selective process; starting from TeCDD it goes in steps to end up with NCDD. The simulated reaction barriers were in the range of 7.95–22.78 kcal/mol and the reaction energies were in the range of 12.06–43.26 kcal/mol. The order obtained from of energy is same as the order predicted by reactivity index calculations. The difference of the reaction energy between TeCDD, DCDD, MCDD and NCDD is almost ∼9.22 kcal/mol. Though the numbers are qualitative, and the energy difference is few kcal/mol, still the trend is in perfect match with the reactivity index results, which proves the utility of reactivity index calculations in designing material. The initial configuration of TeCDD with bidellite cluster is shown in Fig. 6. This is the first step of the decomposition

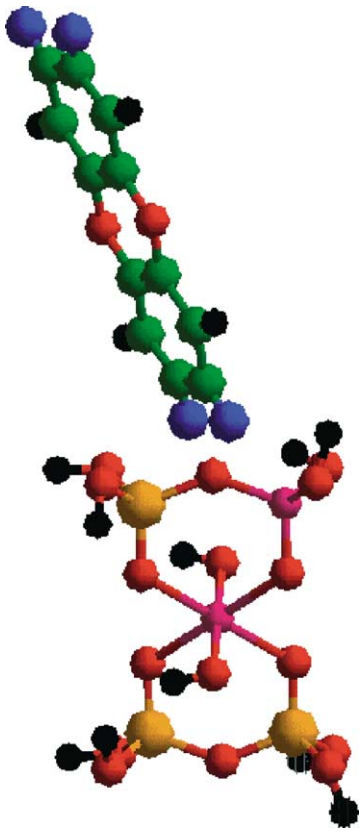

Fig. 6. Initial structure of TeCDD molecule during interaction with aluminum substituted beidellite type clay cluster. The color code is red (oxygen); yellow (silicon); violet (octahedral/tetrahedral aluminum); black (hydrogen); green (carbon); and blue (chlorine).

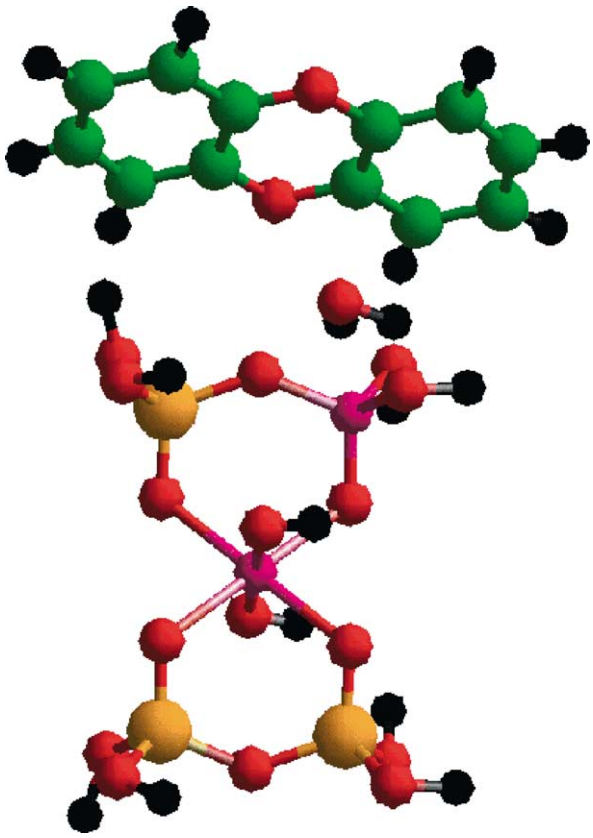

Fig. 7. Initial structure of NCDD molecule during interaction with aluminum substituted beidellite type clay cluster in presence of water. The color code is red (oxygen); yellow (silicon); violet (octahedral/tetrahedral aluminum); black (hydrogen); green (carbon); and blue (chlorine).

process. When the chlorine abstraction is complete, it results in a non-chloro moiety NCDD. Since the dioxin ring remains as such, it may be chlorinated again to lead an enhancement of toxicity. Hence, the decomposition of dioxin ring is the target. Now among the sixteen bonds present in dioxin it looks like the C–O bond breaking is more feasible than C–C bonds because the latter has double bond character due to its presence in the benzene ring. This idea has also been supported by the experimental results probing the formation of dioxin. So there are many debates about the right step but a general consensus has been reached that the dioxin can be generated in the incinerator with direct condensation of its phenoxy radical through TCP [11]. The formation study proposes that formation of dioxin through halo phenols is favored kinetically over the other competing mechanism. Hence, we feel that C–O bond breaking will be the reaction to monitor. The C–O bond breaking process will be triggered by the interaction of NCDD with hydrogen of the clay cluster. The initial configuration is shown in Fig. 7. This reaction will be a two-step process. The first step is that the dioxin oxygen will form a bond with the hydroxyl hydrogen, which will then break away from the oxygen connecting the hydrogen. The second step is the C–O bond breaking. Now, here the addition of a hydrogen radical to the oxygen of NCDD is unlikely since the oxygen atom does not form a three coordinated species like C–OH–C in the neutral state. Thus, a proton should be added to NCDD because a dative bond then can be formed between the oxygen lone pair of NCDD and a proton. After this proton attachment, there is a need of another hydrogen source, which can approach the proton–NCDD complex to break the C–O bond. Prost [38] has proposed that in case of beidellite the water molecules adsorbed in interlamellar spaces are involved in hydrogen bonding with oxygen atoms belonging to tetrahedral SiO_4^- replaced by AlO_4^- tetrahedral. Then, the hydrogen of water molecule will be attracted to the surface hydrogens paving the formation of H_3O^+. We did an exhaustive calculation in our earlier work [17] to show that water may interact with both a structural and hydroxyl hydrogen depending on its location. The interlayer cation has no influence whatsoever in this interaction process. Once the hydronium ion generated, then it can be an active source of hydrogen radical in the medium. It has been also shown in our periodic calculation that for a single water molecule that the influence of sodium is negligible. As in reality, the clay contains the interlayer cation to balance the layer charge generated by octahedral/tetrahedral substitution of Al^{3+}/Si^{4+} by other divalent/trivalent metal cation. This hydronium thus generated

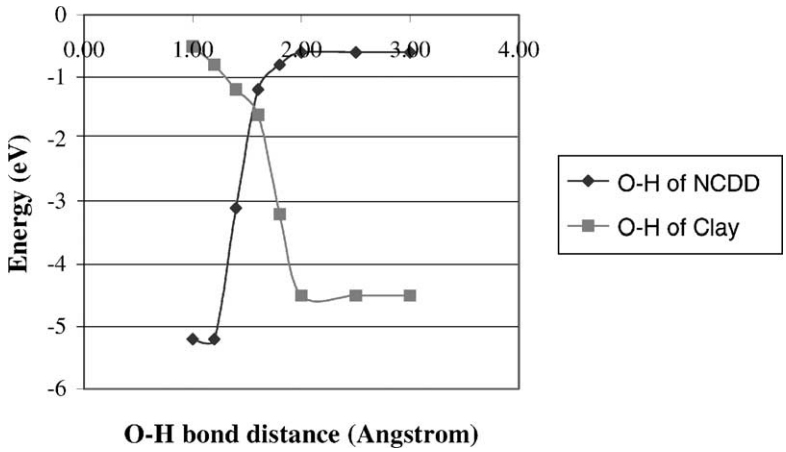

Fig. 8. Potential energy curve to study the feasibility of interaction between hydroxyl proton close to the tetrahedral substitution and the oxygen of NCDD in terms of the O–H bond formation of TCDD and dissociation of O–H bond in the beidellite clay cluster.

will now proceed to the C–O bond breaking phenomenon. This process is as well barrierless. The proton treatment and the C–O bond breaking process are shown in Figs. 8 and 9, respectively. Fig. 8 shows the first formation of a O–H bond between the oxygen center of NCDD, and the hydroxyl hydrogen of the clay cluster, as well as, the bond dissociation of the hydroxyl hydrogen from the oxygen connected with tetrahedral aluminum of the clay cluster. The result shows that the formation of NCDDH is a favorable process, and the stabilization energy is −9.91 kcal/mol, whereas for the availability of hydroxyl hydrogen linked to tetrahedral aluminum the stabilization energy is −106.07 kcal/mol, because the structure stabilizes at a O–H distance of 2 Å. Then, for further distance increments, there is no change in the energy value. The formation of O–H bond in NCDD is stabilized at a O–H distance of 1.2 Å and no further change with

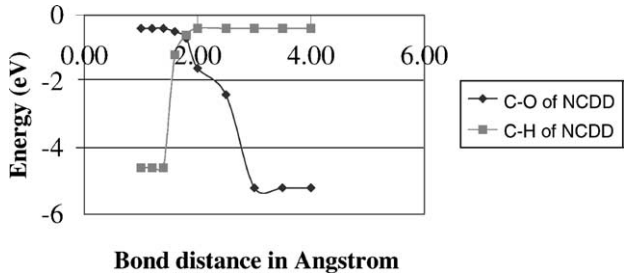

Fig. 9. Potential energy curve to study the feasibility of interaction between hydroxyl proton close to the octahedral substitution and the oxygen of NCDD in terms of the C–O bond breaking of TCDD and formation of C–H bond in NCDD resulting in phenol formation.

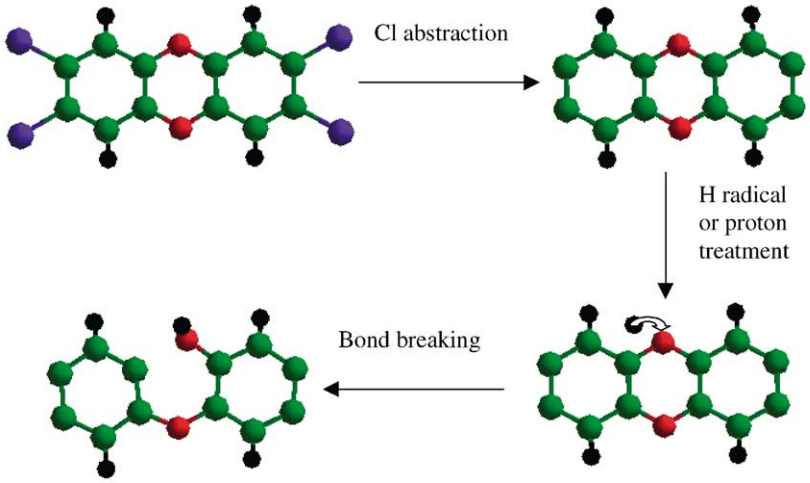

Scheme 1. A schematic diagram to show two step mechanisms, only the interacting molecules are shown. First the chlorine abstraction to form NCDD, then proton attack to NCDD, and finally the bond breaking to form phenol. The color code is red (oxygen); yellow (silicon); violet (octahedral/tetrahedral aluminum); black (hydrogen); green (carbon); and blue (chlorine).

steady decrease in the said distance. Similarly, the next step of the reaction is monitored, and the energetics is shown in Fig. 9. The C–O bond dissociation is stabilized at energy of −5.4 eV at a C–O distance of 3 Å, where as the C–H new bond formation is stabilized at an energy –103.77 kcal/mol at a C–H distance of 1.3 Å. The hydrogen needed for this bond formation is supplied by H_3O^+ ion formed by the interaction of water for a monohydrated clay with surface silanols. This finally results in the formation of phenol, as mentioned by the experimentalist [11] that the formation of dioxin is from the condensation of TCP. So the decomposition of dioxin by the 2:1 smectite family is feasible. The decomposition process is barrierless and consists of two main steps. First, chlorine is abstracted from TeCDD stepwise to form NCDD. Then NCDD interacts with hydroxyl hydrogen to form C–OH–C bond in NCDD. Then, C–O bond breaking occurs in presence of hydronium ion generated in presence of water with its interaction with surface hydroxyls of beidellite. This proposition is shown in Scheme 1.

This solves the long hunt for a material to decompose dioxin. The reactivity indices propose the plausible interaction sites, which help us to design the model and finally the material for the process. Hence, we can use this methodology to design novel materials of interest. The only limitation of this study is the cluster size for the energetics calculation and the absence of interlayer cations. The cluster size is a rational compromise between CPU and accuracy, as stated and observed in our earlier studies [25], and interlayer cations cannot influence hydration as observed before [17]. But still, we wish to pursue this little further using ab initio molecular dynamics to monitor the dynamics of interacting molecules in presence and absence of interlayer cations.

5. Conclusion

This is the first theoretical study to design a suitable inorganic material which is economically and environmentally viable for the effective and selective decomposition of highly hazardous dioxin. The decomposition occurs mainly through two main steps, first chlorine abstraction and second breaking of C–O bond of dioxin. This study compares two common varieties of 2:1 dioctahedral smectite to rationalize an understanding in terms of the activity of hydroxyl hydrogen connected with the octahedral/tetrahedral moiety of the framework which, determines the layer charge of the clay moiety, and hence its catalytic property. The presence of two types of hydroxyl groups is identified in dioctahedral clays, and their role in their respective activity is also rationalized. Finally, beidellite type clays have been chosen due to their immense surface potentiality, which is important in the decomposition process, along with the fact that generation of hydronium ions is feasible in beidellite due to tetrahedral substitution on the surface. This further helps in the C–O bond dissociation process. The comparison is based on reactivity indices, which locates the nucleophilic site of the clay clusters. We then compared these indices with the electrophilicity of dioxin varieties starting from NCDD to TeCDD. The relative nucleophilicity clearly indicated the superiority of beidellite-type of clays. We designed the complexes and performed energy calculation to validate the proposition and also to propose a plausible decomposition mechanism of dioxin. The results showed that the reactivity indices can help to design a new material in terms of their electronic structure. The current methodology can qualitatively locate the active center in a material and the interacting species, which can then be correlated to find a plausible mechanism for a typical reaction. Materials like dioxin are so toxic that experiments are really difficult. The concentration of dioxin in atmosphere is very low to estimate which needs a solid sorbent for concentration and further decomposition as after chlorine abstraction dioxins can be recharged if come into contact with the environment. Our current work involves a wide array of organic toxic pollutants whose pre-concentration with clays will be the cheapest solution of the problem, because the natural occurrence of clay in earth is still plenty. The optimized geometry vividly shows that prediction of pseudo-bond formation between nucleophilic and electrophilic moieties is possible within the helm of HSAB principle. The optimistic results pave the way for expanding the methodology for other systems as well. Simultaneously, the theoretical observation demands experimentation for the materials potential usage, which is under way.

References

[1] R.R. Bumb, W.B. Crummett, S.S. Cutie, J.R. Gledhill, R.H. Hummel, R.O. Kagel, L.L. Lamparski, E.V. Luoma, D.L. Miller, T.J. Nestrick, L.A. Shadoff, R.H. Stehl, J.S. Woods, Science 210 (1980) 385.
[2] F.W. Karasek, F.I. Onuska, Anal. Chem. 54 (1982) 309A.
[3] D.C. Spink, D.W. Lincoln II, H.W. Dickeman, J.F. Gierthy, Proc. Natl. Acad. Sci. U.S.A. 87 (1990) 6917.
[4] K. Tuppurainen, I. Halonen, P. Ruokojarvi, J. Tarhanen, Ruuskanen, J. Chemosphere 36 (1989) 1493.
[5] H.R. Buser, H.P. Bosshardt, C. Rappe, Chemosphere 7 (1978) 165.
[6] K. Olie, P.L. Vermeulen, O. Hutzinger, Chemosphere 6 (1997) 455.
[7] G.A. Eiceman, R.E. Clement, F.W. Karasek, Anal. Chem. 51 (1979) 2343.
[8] E. Wikstrom, S. Marklund, Environ. Sci. Technol. 34 (2000) 604.
[9] N. Ishibashi, K. Yoshihara, K. Nishiwaki, S. Okajima, M. Hirooka, H. Shudo, Organohalogen Compd. 46 (2000) 122.
[10] R. Lujik, D.M. Akkemrman, P. Slot, K. Olie, F. Kapteijn, Environ. Sci. Technol. 28 (1994) 312.
[11] I. Wiater, R. Louw, Eur. J. Org. Chem. (1999) 261.
[12] T. Schaefer, R. Sebastian, THEOCHEM 204 (1990) 41.
[13] J.D. McKinny, K. Chae, E.E. McConell, L.S. Birnbaum, Environ. Health Perspect. 60 (1985) 57.
[14] T. Fuji, K. Tanaka, H. Tokiwa, Y. Soma, J. Phys. Chem. 100 (1996) 4810.
[15] Y. Okamoto, M. Tomonari, J. Phys. Chem. A 103 (1999) 7686.
[16] D.R. Jackson, M.H. Roulier, H.M. Grotta, S.W. Rust, J.S. Warner, in: C. Rappe, G. Choudary, I.H. Keith (Eds.), Chlorinated Dioxins and Dibenzofurans in Perspective, Lewis Publishers, Chelsea, MI, 1986, pp. 185–200.

[17] (a) A. Chatterjee, T. Iwasaki, T. Ebina, J. Phys. Chem. A 104 (2000) 8216, and references therein;
(b) A. Chatterjee, T. Iwasaki, T. Ebina, Comp. Mater. Sci. 14 (1999) 119.
[18] R.G. Pearson, J. Am. Chem. Soc. 105 (1983) 7512.
[19] R.G. Pearson, J. Chem. Educ. 64 (1987) 561.
[20] R.G. Parr, W. Yang, J. Am. Chem. Soc. 106 (1984) 4049.
[21] P. Geerlings, F. De Proft, Int. J. Quant. Chem. 80 (2000) 227.
[22] L.T. Nguyen, T.N. Le, F. De Proft, A.K. Chandra, W. Langenaeker, M.T. Nguyen, P. Geerlings, J. Am. Chem. Soc. 121 (1999) 5992.
[23] W. Langenaeker, F.D. Proft, P. Geerlings, J. Phys. Chem. A 102 (1998) 5944.
[24] A.K. Chandra, P. Geerlings, M.T. Nguyen, J. Org. Chem. 62 (1997) 6419.
[25] A. Chatterjee, T. Iwasaki, T. Ebina, J. Phys. Chem. A 103 (1999) 2489, and references therein.
[26] J.L. Gazquez, F. Mendez, J. Phys. Chem. 98 (1994) 4591.
[27] W. Yang, M.J. Mortier, J. Am. Chem. Soc. 108 (1986) 5708.
[28] R.G. Pearson, R.G. Parr, J. Am. Chem. Soc. 105 (1983) 7512.
[29] W. Kohn, L. Sham, J. Phys. Rev. A 140 (1965) 1133.
[30] A. Becke, J. Chem. Phys. 88 (1988) 2547.
[31] C. Lee, W. Yang, R.G. Parr, Phys. Rev. B 37 (1988) 786.
[32] C.W. Bock, M. Trachtman, J. Phys. Chem. 98 (1994) 95.
[33] S.F. Boys, F. Bernardi, Mol. Phys. 19 (1970) 553.
[34] A. Chatterjee, H. Hayashi, T. Iwasaki, T. Ebina, K. Torii, J. Mol. Catal. A 136 (1998) 195.
[35] R.K. Roy, S. Krishnamurti, P. Geerlings, S. Pal, J. Phys. Chem. A 102 (1998) 3746.
[36] A. Chatterjee, T. Iwasaki, T. Ebina, J. Phys. Chem. A 105 (2001) 10694.
[37] G. Sposito, R. Prost, Chem. Rev. 82 (1982) 553.
[38] R. Prost, A. Koultit, A. Benchara, E. Huard, Clays Miner. 46 (1998) 117.